European Review for Medical and Pharmacological Sciences 2023; 27: 384-394

Development and validation of COVID-19 Radiological Risk Score (COVID-RRS): a multivariable radiological score to estimate the in-hospital mortality risk in COVID-19 patients

W. SCHMIDT[1,2,3], K. PAWLAK-BUŚ[1,2], B. JÓŹWIAK[1,2], K. KATULSKA[4], P. LESZCZYŃSKI[1,2]

[1]Rheumatology and Osteoporosis Ward, J. Strus Municipal Hospital in Poznan, Poznan, Poland
[2]Department of Internal Medicine, [3]Doctoral School, [4]Department of General Radiology and Neuroradiology, Poznan University of Medical Sciences, Poznan, Poland

Abstract. – OBJECTIVE: To develop and validate in-hospital mortality risk score comprising radiological aberrances in chest computed tomography (CT) performed on admission.

PATIENTS AND METHODS: Single-center, longitudinal cohort study in adult patients admitted with Coronavirus Disease 2019 (COVID-19) to our ward. Patients were followed-up during hospitalization until discharge or death. Eligibility criteria for the study comprised positive real-time reverse transcription-polymerase chain reaction test (RT-PCR) for severe acute respiratory syndrome coronavirus 2 (SARS-CoV-2) and ground-glass opacities in chest CT. In-hospital death was the outcome of interest. Radiological, laboratory, and clinical data were analyzed. Radiological determinants of mortality were used as variables in multivariate logistic regression analysis, and results were used to build a radiological risk score.

RESULTS: 371 patients were enrolled in development and validation cohorts (181 and 190 respectively), with a total of 47 non-survivors. Univariate analysis data determined 12 predictive factors (nine risk and three protective). In multivariate analysis, we developed COVID-RRS (COVID-19 Radiological Risk Score) - a radiological score predicting in-hospital COVID-19 mortality risk comprising estimated lung involvement percentage, pleural effusion, and domination of consolidation-type changes in chest CT. Our score was superior in the prediction of COVID-19 mortality to the percentage of lung involvement alone, Chest Computed Tomography Severity Score (CTSS), and Total Severity Score (TSS) in both groups with AUC of 0.910 and 0.902, respectively (p <0.001).

CONCLUSIONS: Additional imaging features independently contribute to COVID-19 mortality risk. Our model comprising lung involvement estimation, pleural effusion, and domination of consolidations performed significantly better than scores based on the extent of the changes alone. COVID-RRS is a simple, reliable, and ready-to-use tool for clinical practice.

Key Words:
COVID-19, SARS-CoV-2, Chest CT.

Introduction

We have been confronting severe acute respiratory syndrome coronavirus 2 (SARS-CoV-2) pandemics for more than two years[1]. Throughout the pandemics, many papers on radiological aspects of Coronavirus Disease 2019 (COVID-19) have been published regarding diagnostics and prognosis in this disease, including an early and thorough review by Ye et al[2] that described frequent and rare chest computed tomography (CT) manifestations of this disease. During the severe COVID-19, typical signs of interstitial pneumonia are present: bilateral ground-glass opacities (GGO) that evolve into consolidations or progress into GGO with marked interstitial septal thickening giving crazy paving pattern later in the disease[3]. Many authors[4-6] developed and tested different lung parenchyma involvement indices, such as chest CT score or total severity score (TSS), assessed by radiologists or artificial intelligence. The complexity of the abovementioned scores varies greatly and extents from

Corresponding Author: Wiktor Schmidt, MD; e-mail: wiktorpawelschmidt@gmail.com

simple estimation in percentage by assessing radiologists through scores assessing every lung lobe or segment separately, such as adapted from severe acute respiratory syndrome coronavirus 1 (SARS-CoV-1), outbreak chest CT severity score (CT-SS) or TSS[5,7]. On the other hand, COVID-19 radiological features comprise many additional signs such as pleural effusion, lymphadenopathy, vascular enlargement, or air bronchogram that can affect prognosis[8]. However, most papers[3-7] focus on either lung involvement or additional features without assessing their independent influence on prognosis.

In our study, we aimed to assess whether adding additional imaging signs to the estimation of lung involvement in computed tomography can improve predicting mortality in COVID-19. We developed and validated a radiological model of in-hospital mortality comprised of an estimation of the extent of interstitial changes and independent radiological variables that occurred in on-admission chest CT in patients hospitalized due to COVID-19.

Patients and Methods

Study Setting and Population

We conducted a single-center, longitudinal cohort study in 371 adult patients admitted with COVID-19 to our ward (secondary care settings in multi-specialty hospital) that has functioned as a COVID-19 facility from March 16th, 2020, to February 28th, 2022. Patients were followed-up during hospitalization on our ward and in ICU, if applicable, until hospital discharge or death. The derivation group was assessed retrospectively, whereas the validation group was prospective. The retrospective cohort was hospitalized between March 16th, 2020, and January 31st, 2021, whereas prospective data were gathered between February 1st and June 16th, 2021 (discharge of the last patient). Eligibility criteria for the study were positive real-time reverse transcription-polymerase chain reaction test (RT-PCR) result for SARS-CoV-2 from the nasopharyngeal swab, and ground-glass opacities present in chest CT performed upon admission to the hospital. The study size was arrived at including all patients hospitalized within the abovementioned time range who were eligible. Patients were treated following local guidelines, which evolved during the study. Oxygen supplementation was given to patients who presented with arterial blood saturation measured with a finger pulse oximeter (SpO_2) <94% on room air, and flow was titrated to achieve SpO_2 95-98%. Patients who deteriorated despite low-flow oxygen supplementation were treated with a high-flow nasal cannula (HFNC). Those who deteriorated despite or did not tolerate it were consulted by anaesthesiologists, who individually qualified patients into treatment in the intensive care unit (ICU). In-hospital death was the outcome of interest. Patients lost to follow-up with missing clinical and laboratory data were excluded from the analysis. The study was developed and described in accordance with the Transparent Reporting of multivariable prediction model for Individual Prognosis or Diagnosis (TRIPOD) guideline[9]. We obtained the local ethical committee of Poznan University of Medical Sciences' opinion of the non-experimental character of our research on February 3rd, 2021, and approval of the study on February 4th, 2021 (consent No. 108/21).

Radiological, Clinical, and Laboratory Assessment

We collected clinical, radiological, and laboratory data available in hospital documentation in a prospective way for the validation cohort and retrospectively with a questionnaire prepared for this research for the development group. Chest CT scans were obtained with the use of Siemens Somatom Sensation 64-slice computed tomography machine (Erlangen, Germany) on admission to the hospital in Emergency Department (ED) or during the transfer from ED to our ward. High resolution chest CT protocol without intravenous contrast was applied – thorax was examined from lung apices to bases, patients were supine and holding breath on maximal inspiration, slice thickness 1.0 mm, 120 kV, 150 mA (with automatic exposure control system), 0.5 s rotation time, pitch 0.9, detector collimation 0.6 mm, kernel B80f, matrix of 512 × 512 mm. The analysis of lung involvement was performed using Frontier Lung Analysis software (Siemens, AG; Healthcare Sector, Erlangen, Germany). The reconstruction with the Br59 kernel was used. The percentage of opacity (total percent of affected lung parenchyma), and percentage of high-volume opacity (using a threshold of -200 Hounsfield unit, HU) were analysed. Pulmonary and mediastinal windows were acquired. Images were assessed by radiologist with >15 years of experience in

chest CT (K. Katulska) and by two internists/rheumatologists with at least ten years of experience in assessing lung CT of patients with interstitial lung diseases (P. Leszczynski, K. Pawlak-Bus). Radiological signs were described following the Fleischner Society glossary[10], and special attention was paid to signs and symptoms described in the early review of COVID-19 chest CT images by Ye et al[2]. Lung involvement was assessed with simple percentage estimation and two radiological scores: chest CT score[7] and Total Severity Score[5]. Ground glass opacities were present in all patients due to being one of the inclusion criteria. Following additional radiological signs were assessed: dominating changes, their pattern and distribution in axial, coronal, and sagittal planes, presence of consolidations, interlobular septal thickening, crazy paving pattern, fibrotic changes, pleural effusion and/or thickening, subpleural curvilinear line, mediastinal and hilar lymphadenopathy, bronchial wall thickening, air bronchogram, vascular enlargement, dilated pulmonary artery (>29 mm), halo sign, reverse halo sign, nodular and polynodular changes, pericardial effusion, air bubble sign, tree-in-bud changes, emphysema, and bronchiectasis[2].

Clinical factors that we extracted included age, sex, body-mass-index (BMI), symptoms, time from symptoms onset to hospital admission, World Health Organization Ordinal Scale[11], heart rate, temperature, SpO_2, oxygen concentration (FiO_2, estimated with the method by Wettstein et al[12]), systolic and diastolic blood pressure (SBP and DBP), respiratory rate (RR), comorbidities and Charleson Comorbidity Index (CCI)[13] and treatment instituted throughout hospitalization. Laboratory data included: complete blood count (CBC), C-reactive protein (CRP), procalcitonin (PCT), interleukin 6 (IL-6), lactate dehydrogenase (LDH), high-sensitive troponin I (hs-TnI) and D-dimer. All analysed clinical and laboratory results were obtained on admission – within the first 48 hours (in ED or on our ward). They were obtained using laboratory analysers (Roche Cobas c501, Siemens ADVIA Centaur CP, Abbott ARCHITECT i1000SR, Sysmex XN-100,0, and Werfen ACL Top 700).

Statistical Analysis

We conducted the statistical analysis with PQStat v.1.8.2. We used the Chi-square test to compare categorical data under the condition that Cochrane's rule was applicable; when it was not, and the expected frequency was small, Fisher's exact test was used. Ordinal and continuous data without normal distribution were analysed with the Mann-Whitney U test, whereas continuous data with normal distribution was evaluated with the *t*-Student test (the equality of variances rule was satisfied). Subsequently, univariate logistic regression was applied to radiological covariates to achieve unadjusted odds ratios. Afterward, we performed multivariate binary stepwise logistic regression using obtained risk and protective factors as dependent categorical variables. We identified independent predictors of COVID-19 in-hospital mortality using the backward elimination method (predictors with a $p > 0.05$ were removed). Interactions between the radiological variables were considered before building the model. Calibration was assessed with the Hosmer and Lemeshow "goodness of fit" test. Internal validation was performed with the use of 10-fold cross-validation. Then, we derived the COVID-19 Radiological Risk Score (COVID-RRS) *via* simplifying β coefficients from the model. Performance and discrimination were evaluated *via* area under curve (AUC) analysis of the receiver operating characteristic (ROC) curve and the estimated ROC curve of the model (DeLong's method). A comparison of AUCs in ROC curves of derived COVID-RRS and scores mentioned in the previous section (percentage lung involvement estimation, chest CT score, and TSS) was also performed with DeLong's method. Cut-off points were obtained with the Youden index. We defined statistical significance with a *p*-value equal to or less than 0.05.

Results

Three hundred seventy-one patients hospitalized in our ward were eligible, and we included them in the study. Due to organizational issues, four patients in the development cohort and two patients in the validation group needed to be transferred to other non-ICU wards and were excluded from the study due to missing data in the follow-up. The rest was followed-up throughout hospitalization. The participant flow diagram is presented in Figure 1.

Descriptive characterization of derivation and validation groups is presented in Table I. Patients from development and validation groups

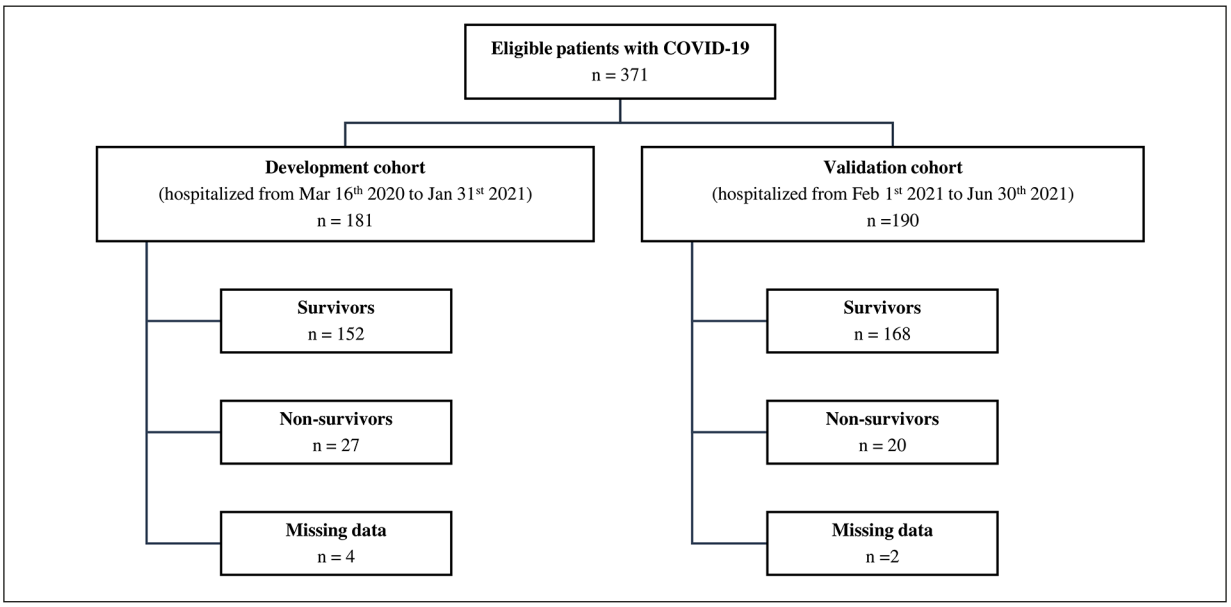

Figure 1. Participant flow diagram of the study.

differed not only in comorbidity burden measured with CCI but also in the type of comorbidities – more patients in the development group had heart failure (8 *vs.* 2) and end-stage chronic kidney disease (3 *vs.* 0). Groups did not differ significantly in the prevalence of hypertension, chronic kidney disease, ischaemic heart disease, diabetes mellitus, connective tissue disorders, transplant recipients, asthma/COPD, neoplastic disease, and inflammatory bowel disease. Patients between development and validation groups also differed in instituted treatment, predominantly due to the availability of treatment options and evolution of treatment schedules throughout pandemics. In both groups steroids, remdesivir, and tocilizumab were broadly used (135 patients in the development and 185 patients in the validation group received GCS, respectively, 108 and 146 were treated with remdesivir, whereas 55 and 85 patients also had treatment with tocilizumab instituted). In the development cohort, 32 patients additionally received chloroquine and 6 – lopinavir/ritonavir (LPV/RTV). Both drugs were not used in the validation cohort. More patients in the development group were also treated with convalescent plasma (104 *vs.* 7). Almost all patients in both groups received prophylaxis with anticoagulants, predominantly low-molecular-weight heparins (LMWH, 168 patients in the development group and 183 in the validation cohort), and others received unfractionated heparin (UHF, 2 and 4 respectively) or new oral anticoagulants (NOACs, 7 and 1 respectively). Twenty-eight patients in the development and 35 in the validation group also received antiplatelet agents (mainly acetylsalicylic acid and clopidogrel).

The radiologic characteristics of study participants are presented in Table II. Signs that were seen only occasionally were not presented, and they comprise reverse halo sign (1 patient in development group), polynodular changes (2 patients in development and 1 in validation group), pericardial effusion (13 patients in development and 4 in validation group), air bubble sign (8 and 2 patients respectively) and tree-in-bud changes (1 patient in each group).

In a univariate analysis made with logistic regression, we encountered 12 radiological determinants of COVID-19 in-hospital mortality, which are presented in Table III.

Covariates obtained in the unadjusted analysis were then used to develop the predictive model in multivariate logistic regression (Table IV) and then to derive calculator of COVID-RRS (COVID-19 Radiological mortality Risk Score), specified in Table V.

The performance of our index in both groups is presented in Figure 2. The optimal cut-off point derived from the Youden index was 5.5 points in both groups, and in each group had excellent sensitivity with good specificity.

Table I. Descriptive characterization of development and validation groups; N (%), median (Q1-Q3) or mean (± SD).

Characteristic	Development group			Validation group		
	Survivors n = 152 (84.9%)	Non-survivors n = 27 (15.1%)	*p*	Survivors n = 168 (89.4%)	Non-survivors n = 20 (10.7%)	*p*
Age (years)	59.8 (± 14.4)	68.8 (± 15.0)	0.003*	58.1 (± 14.6)	65.6 (± 12.3)	0.028*
Sex (male)	82 (54.7%)	15 (55.6%)	0.932**	102 (60.7%)	12 (60.0%)	0.951**
BMI (kg/m^2)	28.0 (24.8-32.7)	30.0 (25.9-34.1)	0.245***	28.1 (24.8-32.4)	29.2 (25.3-32.2)	0.769***
Time from onset (d)	8.0 (6.3-11.0)	5.5 (5.0-10.0)	0.033***	8.0 (6.0-10.0)	5.0 (3.5-9.0)	0.021***
WHO Ordinal Scale:						
4	18 (12.0%)	-	0.079****	28 (16.7%)	2 (10.0%)	0.746****
5	132 (88.0%)	27 (100.0%)	0.079****	140 (83.3%)	18 (90.0%)	0.746****
SpO_2/FiO_2	180 (121-262)	116 (112-121)	< 0.001***	254 (179-443)	116 (108-138)	< 0.001***
RR	14 (12-18)	20 (16-24)	< 0.001***	14 (12-18)	20 (18-23)	< 0.001***
CCI	2 (1-4)	5 (3-6)	< 0.001***	0 (0-1)	0 (0-4)	0.062***
Lab parameters:						
CRP [mg/l]	66.7 (34.8-116.8)	110.6 (48.9-189.4)	0.018***	69.5 (36.1-134.3)	143.5 (43.6-238.9)	0.035***
PCT [ng/ml]	0.06 (0.04-0.11)	0.16 (0.08-0.82)	< 0.001***	0.06 (0.03-0.10)	0.20 (0.07-0.80)	< 0.001***
IL-6 [pg/ml]	36.0 (17.2-75.8)	87.5 (57.4-198.1)	< 0.001***	40.8 (21.7-75.2)	62.5 (39.5-171.1)	0.010***
WBC [G/l]	6.4 (5.0-8.1)	7.8 (5.1-11.4)	0.106***	6.0 (4.6-7.8)	8.1 (5.8-10.2)	0.005***
PLT [G/l]	215 (163-288)	199 (155-254)	0.243***	206 (163-287)	201 (146-278)	0.773***
LDH [U/l]	324 (259-439)	508 (386-717)	< 0.001***	372 (282-462)	507 (421-689)	0.001***
hs-TnI [ng/l]	11.0 (6.0-19.5)	25.0 (11.5-52.0)	0.003***	9.0 (6.0-20.0)	12.0 (7.5-31.5)	0.111***
D-dimer [µg/ml]	0.76 (0.48-1.32)	1.53 (1.05-2.48)	< 0.001***	0.77 (0.52-1.25)	1.45 (0.89-2.68)	0.001***

t*-Student test, **Chi-square test, ***Mann-Whitney U-Test, ** Fisher's exact test. Body mass index (BMI), World Health Organization (WHO), arterial blood saturation measured with finger pulse oximeter (SpO_2), oxygen concentration (FiO_2), Respiratory Rate (RR), Charleson Comorbidity Index (CCI), C-reactive protein (CRP), procalcitonin (PCT), inteleukin-6 (IL-6), white blood cells count (WBC), platelet count (PLT), lactate dehydrogenase (LDH), high specific troponin I (hs-TnI).

Table II. Radiologic signs and differences between survivors and non-survivors in development and validation groups; N (%) or median (Q1-Q3).

Characteristic	Development group			Validation group		
	Survivors n = 152 (84.9%)	Non-survivors n = 27 (15.1%)	p	Survivors n = 168 (89.4%)	Non-survivors n = 20 (10.7%)	p
Lung involvement (%)	40 (25-50)	80 (68-88)	< 0.001*	30 (25-50)	75 (55-85)	< 0.001*
Lung involvement (chest CT score)	10 (6-13)	20 (17-22)	< 0.001*	8 (6-13)	19 (14-21)	< 0.001*
Lung involvement (TSS)	8 (5-10)	16 (14-18)	< 0.001*	6 (5-10)	15 (11-17)	< 0.001*
Dominating changes:						
Ground glass opacities	97 (54.8%)	21 (11.9%)	0.183**	130 (76.0%)	18 (94.7%)	0.079***
Consolidations	48 (27.1%)	2 (1.1%)	0.009**	39 (22.8%)	1 (5.3%)	0.082***
Other	5 (2.8%)	4 (2.3%)	0.012***	2 (1.2%)	0 (0.0%)	1.000***
Pattern:						
Peripheral	80 (45.2%)	3 (1.7%)	< 0.001**	115 (67.3%)	5 (26.32%)	< 0.001**
Diffuse	4 (2.3%)	23 (13.0%)	< 0.001**	53 (31.0%)	14 (73.7%)	< 0.001**
Central	3 (1.7%)	1 (3.7%)	0.487***	4 (2.3%)	-	1.000***
Rrandom	3 (1.7%)	-	1.000***	-	-	-
Distribution (sagittal plane)						
Anterior	3 (2.0%)	0 (0.0%)	1.000***	1 (0.6%)	-	1.000***
Posterior	143 (95.3%)	27 (100.0%)	0.597***	169 (98.8%)	19 (100.0%)	1.000***
Distribution (coronal plane)						
Lower	106 (70.7%)	24 (88.9%)	0.048**	144 (84.2%)	19 (100.0%)	0.081***
Middle	28 (18.7%)	2 (7.4%)	0.557***	20 (11.7%)	-	0.229***
Upper	10 (6.7%)	1 (3.7%)	0.151***	5 (2.9%)	-	1.000***
Consolidations	110 (73.3%)	18 (66.7%)	0.476**	130 (76.0%)	14 (73.7%)	0.783***
Interlobular septal thickening	82 (54.7%)	18 (66.7%)	0.247**	106 (62.0%)	12 (63.2%)	0.921**
Crazy paving	9 (6.0%)	6 (22.2%)	0.014***	1 (0.6%)	-	1.000***
Fibrotic changes	67 (44.7%)	6 (22.2%)	0.029**	60 (35.1%)	2 (10.6%)	0.030**
Pleural effusion	16 (10.7%)	8 (29.6%)	0.014***	5 (2.9%)	5 (26.3%)	0.001***
Pleural thickening	14 (9.3%)	3 (11.1%)	0.727***	2 (1.2%)	1 (5.3%)	0.272***
Subpleural curvilinear line	20 (13.3%)	1 (3.7%)	0.206***	25 (14.6%)	-	0.083***
Mediastinal lymphadenopathy	31 (20.7%)	11 (40.7%)	0.024**	25 (14.6%)	7 (36.8%)	0.023***
Hilar lymphadenopathy	6 (4.0%)	6 (22.2%)	0.004***	6 (3.5%)	2 (10.5%)	0.184***
Bronchial wall thickening	47 (31.3%)	9 (33.3%)	0.837**	23 (13.5%)	5 (26.3%)	0.166***
Air bronchogram	39 (26.0%)	20 (74.1%)	< 0.001**	59 (34.5%)	17 (89.5%)	< 0.001**
Vascular enlargement	40 (26.7%)	16 (59.3%)	< 0.001**	33 (19.3%)	11 (59.1%)	< 0.001**
Dilated pulmonary artery	80 (53.3%)	22 (81.4%)	0.006**	1 (0.6%)	1 (5.3%)	0.190***

*Mann-Whitney U-Test, **Chi-square test, ***Fisher's exact test; computed tomography (CT), Total Severity Score (TSS).

Table III. Prognostic factors of COVID-19 mortality identified in univariate analysis.

Risk factor	OR	95% CI	*p*
> 60% involved lung parenchyma	23.10	7.97-66.99	< 0.001
Diffuse changes	8.39	2.76-25.47	< 0.001
Air bronchogram	8.13	3.19-20.71	< 0.001
Hilar lymphadenopathy	6.86	2.02-23.24	0.002
Crazy paving	4.48	1.45-13.86	0.016
Vascular enlargement around lesions	4.00	1.71-9.35	0.001
Dilated pulmonary artery	3.85	1.38-10.71	0.012
Pleural effusion	3.52	1.33-9.35	0.019
Mediastinal lymphadenopathy	2.64	1.11 -6.26	0.024
Fibrosis	0.35	0.14-0.92	0.049
Dominating consolidations	0.17	0.04-0.75	0.009
Peripheral changes	0.11	0.03-0.38	< 0.001

Odds ratio (OR), 95% confidence interval (95% CI).

Table IV. Independent risk factors obtained with logistic regression analysis, summary of the model and point attribution to COVID-19 Radiological Risk Score (COVID-RRS).

Risk factor	aOR	95% CI	*p*	β	95% CI	SE	Wald	df	Attributed score in COVID-RRS
Estimated lung involvement (%)	1.09	1.04-1.14	< 0.001	0.09	0.04-0.14	0.025	13.04	1	× 0.1
Pleural effusion	3.13	1.39-7.01	0.006	1.14	0.33-1.95	0.41	10.31	1	+ 1
Dominating consolidations	0.39	0.15-0.99	0.049	-0.93	-1.87-(-0.01)	0.48	9.48	1	- 1
Summary of the model									
Wald test	$p < 0.001$								
Cox-Snell R^2	0.33								
Nagelkerk R^2	0.58								
Likelihood Ratio	-39.76								
Hosmer-Lemeshow test	$p = 0.9966$								
AUC	0.935								
Estimated AUC	0.848								

Adjusted odds ratio (aOR), 95% confidence interval (95% CI), standard error (SE), degrees of freedom (df), COVID-19 Radiological Risk Score (COVID-RRS), area under curve (AUC).

COVID-RRS in derivation and validation cohort performed better than indices based solely on lung involvement – comparison of ROC curves of our index and simple percentage estimation of lung involvement is presented in Figure 3. It also outperformed TSS (AUC 0.910 *vs.* 0.881 in development cohort, 0.902 *vs.* 0.874 in validation cohort, $p = 0.026$ and 0.022) and chest CT score (AUC 0.910 *vs.* 0.879 in derivation group and 0.902 *vs.* 0.873 in validation group, $p = 0.031$ and 0.029, respectively).

Table V. COVID-19 Radiological Risk Score (COVID-RRS).

Variable	Score
Estimated lung parenchyma involvement extent (%)	× 0.1
Presence pleural effusion	+ 1
Domination of consolidations in the pattern	- 1

Discussion

In our study, we developed COVID-RRS, radiological risk score for predicting in-hospital mortality made from alternations in chest CT of patients admitted due to COVID-19. The score is easy to perform and is constructed with frequently reported radiological signs: estimated lung involvement, presence of pleural effusion, and dominating changes. We validated the score pro-

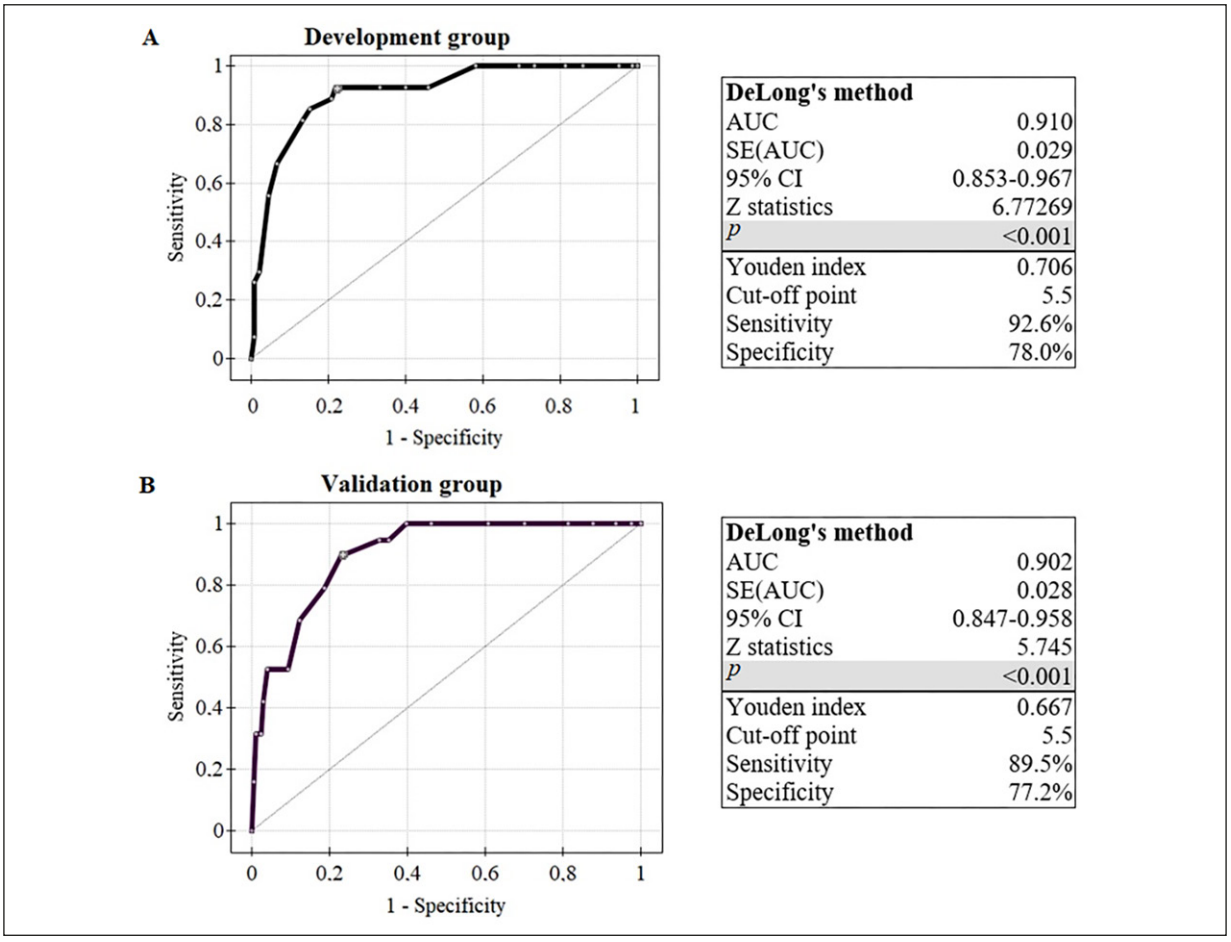

Figure 2. COVID-RRS performance - ROC curves and cut-off points in mortality prediction in development (**A**) and validation (**B**) cohort.

spectively and proved that it performs better than scores based on sole lung involvement extent. Its performance did not differ between development and validation cohorts. Thus, we proved that additional radiological features contribute independently to COVID-19 mortality prognosis. We believe that this simple tool can be readily used in clinical practice after further broad validation by other investigators to make it fully reliable. We also found twelve prognostic factors previously described as predictive of mortality in COVID-19, proving their significance.

Radiological assessment is necessary for COVID-19 severity and prognosis assessment. Risk scores of lung involvement estimation, such as CTSS, chest CT score, and TSS, were constructed and validated, proving their utility in COVID-19 mortality estimation[5,7,14-17]. Modification of TSS (mTSS) with adding qualitative data (type of dominating pattern) was also described[18]. The prognostic potential of additional radiological factors such as diffuse changes, crazy-paving pattern[19], or pleural effusion[20] was also described broadly elsewhere. Some authors combined CT features with clinical and laboratory ones. Khosravi et al[17] developed a model comprising lung involvement, reticular pattern, anemia, and age ≥65. Koch et al[21] developed a radiological score with chest CT opacity score and coronary artery calcium score that performed better than any of the composites separately, emphasizing that even extra-pulmonary imaging features contribute to COVID-19 prognosis. Elmokadem et al[14] proved that combining TSS with the qualitatively assessed pattern of changes (mTSS) improved its specificity in discrimination of severe/critical patients. Our model, based solely on respiratory system alternations in chest CT, enables thorough radiological mortality risk assessment.

External validation and reliability of COVID-RRS make it a simple, quick, and ready-to-use tool for clinicians working with COVID-19 patients. Its

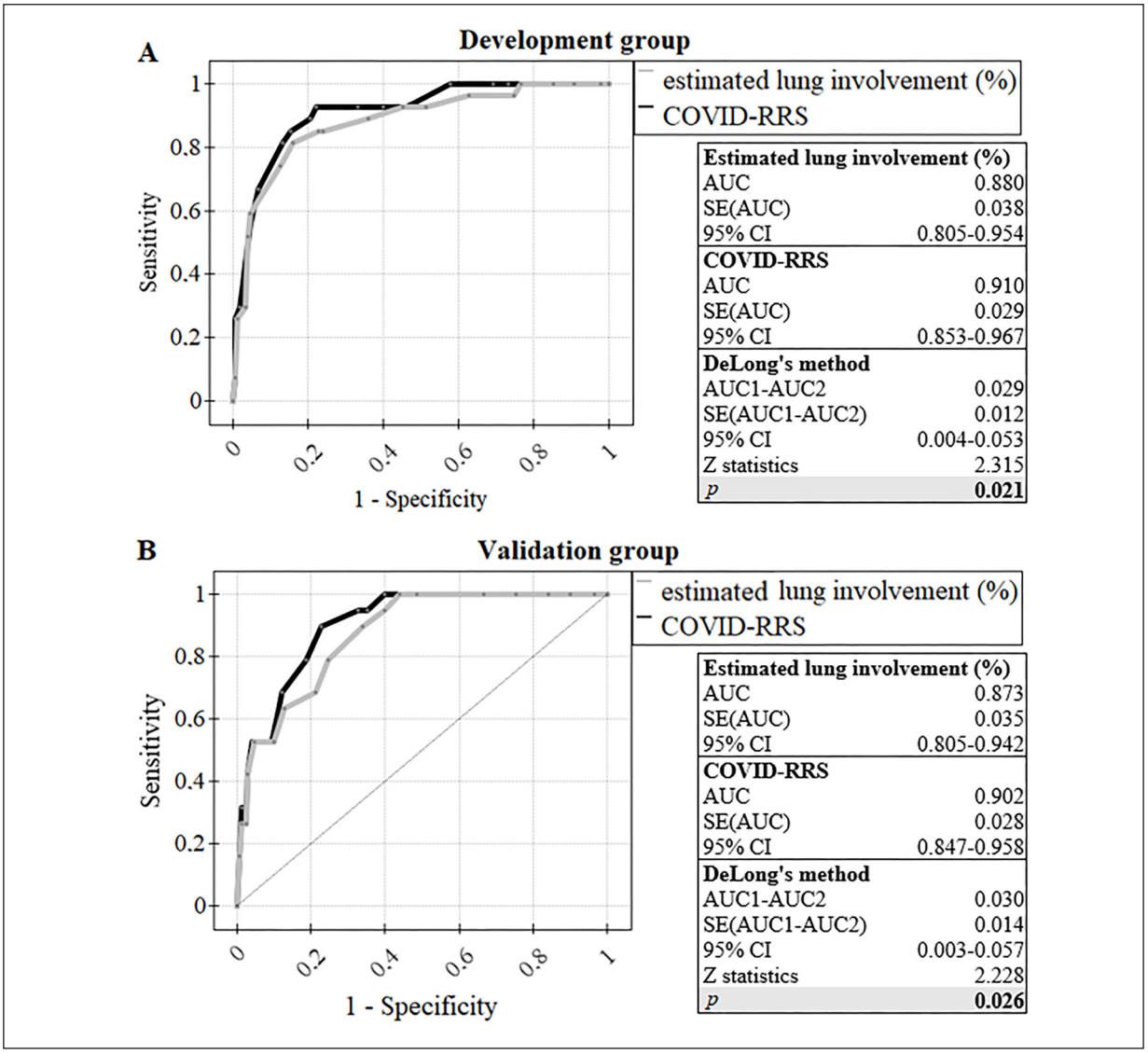

Figure 3. Comparison of ROC curves of COVID-RRS and estimated lung involvement (%) in mortality prediction in development (**A**) and validation (**B**) group.

simplicity should be emphasized as it comprises frequently reported radiological signs in real-life conditions. Qualitative analysis's importance was also proved by finding significant independent variables affecting prognosis. Development and validation cohorts differed in time and, consequently in dominating variants. This proves potential reliability in different waves of pandemics.

Limitations

Limitations of our study comprise single-center character and reliance on reports by a single radiologist. Due to the limited study group, we focused on frequent radiological features in the developed model without clinical and laboratory parameters taken into regression analysis. Additional atypical and rarer radiological signs described by authors such as Chen et al[22] also need to be taken into consideration in COVID-19 patients which needs larger study groups.

Given the abovementioned limitations, COVID-RRS reproducibility ought to be externally assessed optimally in a multi-center study. Performance of our score can also be studied with different endpoints such as ICU admission or long-term prognosis and mortality. Development of new and validation of existing radiological risk scores should be optimally studied in larger study groups. Finally, the performance of COVID-RRS

and other prognostic indices in the younger population could be assessed.

Conclusions

In our study, we proved that adding additional imaging features to lung involvement extent in chest CT on admission improves prognostic performance. We created COVID-RRS, a simple, reliable, and ready-to-use clinical practice tool to enhance radiological risk assessment in COVID-19 patients.

Conflict of Interest
The Authors declare that they have no conflict of interests.

Acknowledgements
We would like to thank our colleagues Zofia Czabajska, Katarzyna Wiśniewska, Cezary Iwaszkiewicz, Magdalena-Owczarek-Bacic, Paula Kaczmarek, Alina Podkowińska and Mateusz Kokot for their support in data gathering.

Funding
No funding was obtained for this study.

Authors' Contribution
All authors participated in conception and design of the study. Acquisition of data was performed by Barbara Jóźwiak and Wiktor Schmidt. Data were interpreted by Katarzyna Katulska and analyzed by Wiktor Schmidt. Wiktor Schmidt and Barbara Jóźwiak were responsible for drafting the article, whereas Katarzyna Katulska, Katarzyna Pawlak-Buś and Piotr Leszczyński made critical revisions. Piotr Leszczyński and Katarzyna Pawlak-Buś supervised the whole project. All authors collectively made final approval of the version of the article to be published.

Ethics Approval
Authors obtained the local ethical committee of Poznan University of Medical Sciences' opinion of the non-experimental character of our research on February 3rd, 2021, and approval of the study on February 4th, 2021 (consent No. 108/21).

Informed Consent
Informed consents from patients that participated in the study were obtained in accordance with the abovementioned ethical committee recommendations.

ORCID ID
Wiktor Schmidt: 0000-0002-9409-9827; Katarzyna Pawlak-Buś: 0000-0002-1982-5980; Barbara Jóźwiak: 0000-0002-7668-4221; Katarzyna Katulska: 0000-0002-8717-0939; Piotr Leszczyński: 0000-0003-2174-8811.

Availability of Data
Data are available upon request to corresponding author.

References

1) Zhu N, Zhang D, Wang W, Li X, Yang B, Song J, Zhao X, Huang B, Shi W, Lu R, Niu P, Zhan F, Ma X, Wang D, Xu W, Wu G, Gao GF, Tan W. A Novel Coronavirus from Patients with Pneumonia in China, 2019. N Engl J Med 2020; 382: 727-733.
2) Ye Z, Zhang Y, Wang Y, Huang Z, Song B. Chest CT manifestations of new coronavirus disease 2019 (COVID-19): a pictorial review. Eur Radiol 2020; 30: 4381-4389.
3) Bernheim A, Mei X, Huang M, Yang Y, Fayad ZA, Zhang N, Diao K, Lin B, Zhu X, Li K, Li S, Shan H, Jacobi A, Chung M. Chest CT Findings in Coronavirus Disease-19 (COVID-19): Relationship to Duration of Infection. Radiology 2020; 295: e200463.
4) Chaganti S, Grenier P, Balachandran A, Chabin G, Cohen S, Flohr T, Georgescu B, Grbic S, Liu S, Mellot F, Murray N, Nicolaou S, Parker W, Re T, Sanelli P, Sauter AW, Xu Z, Yoo Y, Ziebandt V, Comaniciu D. Automated Quantification of CT Patterns Associated with COVID-19 from Chest CT. Radiol Artif Intell 2020; 2: e200048.
5) Li K, Fang Y, Li W, Pan C, Qin P, Zhong Y, Liu X, Huang M, Liao Y, Li S. CT image visual quantitative evaluation and clinical classification of coronavirus disease (COVID-19). Eur Radiol 2020; 30: 4407-4416.
6) Chang YC, Yu CJ, Chang SC, Galvin JR, Liu HM, Hsiao CH, Kuo PH, Chen KY, Franks TJ, Huang KM, Yang PC. Pulmonary sequelae in convalescent patients after severe acute respiratory syndrome: evaluation with thin-section CT. Radiology 2005; 236: 1067-1075.
7) Li K, Wu J, Wu F, Guo D, Chen L, Fang Z, Li C. The Clinical and Chest CT Features Associated With Severe and Critical COVID-19 Pneumonia. Invest Radiol 2020; 55: 327-331.
8) Tabatabaei SMH, Talari H, Moghaddas F, Rajebi H. CT Features and Short-term Prognosis of COVID-19 Pneumonia: A Single-Center Study from Kashan, Iran. Radiol Cardiothorac Imaging 2020; 2: e200130.
9) Collins GS, Reitsma JB, Altman DG, Moons KGM. Transparent Reporting of a multivariable prediction model for Individual Prognosis or Diagnosis (TRIPOD): the TRIPOD statement. Ann Intern Med 2015; 162: 55-63.

10) Hansell DM, Bankier AA, MacMahon H, McLoud TC, Müller NL, Remy J. Fleischner Society: glossary of terms for thoracic imaging. Radiology 2008; 246: 697-722.
11) WHO Working Group on the Clinical Characterisation and Management of COVID-19 infection. A minimal common outcome measure set for COVID-19 clinical research. Lancet Infect Dis 2020; 20: e192-e197.
12) Wettstein RB, Shelledy DC, Peters JI. Delivered oxygen concentrations using low-flow and high-flow nasal cannulas. Respir Care 2005; 50: 604-609.
13) Charlson ME, Pompei P, Ales KL, MacKenzie CR. A new method of classifying prognostic comorbidity in longitudinal studies: development and validation. J Chronic Dis 1987; 40: 373-383.
14) Elmokadem AH, Mounir AM, Ramadan ZA, Elsedeiq M, Saleh GA. Comparison of chest CT severity scoring systems for COVID-19. Eur Radiol 2022; 32: 3501-3512.
15) Yang R, Li X, Liu H, Zhen Y, Zhang X, Xiong Q, Luo Y, Gao C, Zeng W. Chest CT Severity Score: An Imaging Tool for Assessing Severe COVID-19. Radiol Cardiothorac Imaging 2020; 2: e200047.
16) Pan F, Ye T, Sun P, Gui S, Liang B, Li L, Zheng D, Wang J, Hesketh RL, Yang L, Zheng C. Time Course of Lung Changes at Chest CT during Recovery from Coronavirus Disease 2019 (COVID-19). Radiology 2020; 295: 715-721.
17) Khosravi B, Aghaghazvini L, Sorouri M, Naybandi Atashi S, Abdollahi M, Mojtabavi H, Khodabakhshi M, Motamedi F, Azizi F, Rajabi Z, Kasaeian A, Sima AR, Davarpanah AH, Radmard AR. Predictive value of initial CT scan for various adverse outcomes in patients with COVID-19 pneumonia. Heart Lung 2021; 50: 13-20.
18) Wasilewski PG, Mruk B, Mazur S, Półtorak-Szymczak G, Sklinda K, Walecki J. COVID-19 severity scoring systems in radiological imaging - a review. Pol J Radiol 2020; 85: e361-e368.
19) Pan F, Zheng C, Ye T, Li L, Liu D, Li L, Hesketh RL, Yang L. Different computed tomography patterns of Coronavirus Disease 2019 (COVID-19) between survivors and non-survivors. Sci Rep 2020; 10: 11336.
20) Zhan N, Guo Y, Tian S, Huang B, Tian X, Zou J, Xiong Q, Tang D, Zhang L, Dong W. Clinical characteristics of COVID-19 complicated with pleural effusion. BMC Infect Dis 2021; 21: 176.
21) Koch V, Gruenewald LD, Albrecht MH, Eichler K, Gruber-Rouh T, Yel I, Alizadeh LS, Mahmoudi S, Scholtz JE, Martin SS, Lenga L, Vogl TJ, Nour-Eldin NEA, Bienenfeld F, Hammerstingl RM, Graf C, Sommer CM, Hardt SE, Mazziotti S, Ascenti G, Versace GA, D'Angelo T, Booz C. Lung Opacity and Coronary Artery Calcium Score: A Combined Tool for Risk Stratification and Outcome Prediction in COVID-19 Patients. Acad Radiol 2022; 29: 861-870.
22) Chen Q, Guo L-H, Xia G-J, Wang B, Li J, Kuang H-M, Wang M. The atypical imaging findings of novel coronavirus pneumonia (COVID-19) and its evolution. Eur Rev Med Pharmacol Sci 2021; 25: 1080-1086.